

Linear multistep methods for integrating reversible differential equations

N. Wyn Evans¹ and Scott Tremaine²

¹Theoretical Physics, University of Oxford, 1 Keble Road,
Oxford OX1 3NP, England

²Princeton University Observatory, Peyton Hall, Princeton, NJ 08544, USA

ABSTRACT

This paper studies multistep methods for the integration of reversible dynamical systems, with particular emphasis on the planar Kepler problem. It has previously been shown by Cano & Sanz-Serna that reversible linear multisteps for first-order differential equations are generally unstable. Here, we report on a subset of these methods – the *zero-growth methods* – that evade these instabilities. We provide an algorithm for identifying these rare methods. We find and study all zero-growth, reversible multisteps with six or fewer steps. This select group includes two well-known second-order multisteps (the trapezoidal and explicit midpoint methods), as well as three new fourth-order multisteps – one of which is explicit. Variable timesteps can be readily implemented without spoiling the reversibility. Tests on Keplerian orbits show that these new reversible multisteps work well on orbits with low or moderate eccentricity, although at least 100 steps/radian are required for stability.

1. Introduction

The success of symplectic integration algorithms (SIAs) as tools for the numerical solution of Hamiltonian systems illustrates the importance of numerical algorithms that inherit the fundamental physical constraints of the systems to which they are applied (“geometric integrators”).

Time-reversal symmetry plays a central role in physics (e.g., Davies 1974). To define reversibility formally and without reference to coordinates, let x denote the state of the system governed by the differential equations

$$\frac{dx}{dt} = f(x). \quad (1)$$

Let T be an involution, i.e. an operator such that $T^2x = x$. The system (1) is T -reversible if T reverses the direction of time, that is, if

$$\frac{dTx}{dt} = -f(Tx). \quad (2)$$

In standard phase space $x = (\mathbf{q}, \mathbf{p})$ and $T = \text{diag}(1, -1)$.

The trajectory of the system governed by the differential equations (1) is defined by a map G_t such that a system located at x at time 0 is found at $G_t x$ at time t ; by definition $G_t = G_{-t}^{-1}$. Then, T -reversibility implies that

$$G_t T G_t = T \quad \text{or} \quad T G_t = G_t^{-1} T = G_{-t} T. \quad (3)$$

Reversible systems may or may not be Hamiltonian. However, the general features of motion in reversible and Hamiltonian systems show many similarities, including the existence of families of KAM tori (e.g., Moser 1973; Arnold 1984; Roberts & Quispel 1992). These considerations motivate us to examine reversible integration algorithms (RIAs). A one-step numerical integration algorithm with timestep h is defined by an operator \tilde{G}_h that is intended to be a close approximation to G_h , and the algorithm is an RIA if when it is applied to a reversible system

$$\tilde{G}_h T \tilde{G}_h = T. \quad (4)$$

Note that in contrast to G_t , \tilde{G}_h is not necessarily equal to \tilde{G}_{-h}^{-1} .

1.1. Symplectic integration algorithms

Let us first briefly review SIAs; for more detail see Channell & Scovel (1990), Yoshida (1993), Marsden et al. (1996), and Sanz-Serna & Calvo (1994). The standard example of a Hamiltonian system is motion in a conservative potential (this is also reversible). The Hamiltonian is

$$H(\mathbf{q}, \mathbf{p}) = \frac{1}{2}\mathbf{p}^2 + U(\mathbf{q}) \quad (5)$$

and the equations of motion are

$$\frac{d\mathbf{q}}{dt} = \mathbf{p}, \quad \frac{d\mathbf{p}}{dt} = -\nabla U, \quad (6)$$

or

$$\frac{d^2\mathbf{q}}{dt^2} = -\nabla U. \quad (7)$$

The most popular SIA for such systems is the leapfrog or Verlet algorithm (e.g., Hockney & Eastwood 1981). This is a map from the phase-space coordinates $(\mathbf{q}_n, \mathbf{p}_n)$ at time t_n to coordinates $(\mathbf{q}_{n+1}, \mathbf{p}_{n+1})$ at time $t_{n+1} = t_n + h$, defined by

$$\mathbf{q}' = \mathbf{q}_n + \frac{1}{2}h\mathbf{p}_n, \quad \mathbf{p}_{n+1} = \mathbf{p}_n - h\nabla U(\mathbf{q}'), \quad \mathbf{q}_{n+1} = \mathbf{q}' + \frac{1}{2}h\mathbf{p}_{n+1}. \quad (8)$$

Leapfrog is an explicit second-order method (i.e. the one-step error is $O(h^3)$), but higher-order explicit SIAs can be constructed by concatenating leapfrog steps of different sizes, including backwards steps. Leapfrog can be generalized to any separable Hamiltonian of the form $H = \sum H_j$ where each H_j is integrable.

For general Hamiltonians, SIAs can be constructed by two methods. The first is based on expanding the scalar generating functions for the symplectic transformation $(\mathbf{q}_n, \mathbf{p}_n) \rightarrow (\mathbf{q}_{n+1}, \mathbf{p}_{n+1})$ in powers of h (Kang 1986; Channell & Scovel 1990). The simplest example is the first-order SIA

$$\mathbf{q}_{n+1} = \mathbf{q}_n + h \frac{\partial H(\mathbf{q}_n, \mathbf{p}_{n+1})}{\partial \mathbf{p}_{n+1}}, \quad \mathbf{p}_{n+1} = \mathbf{p}_n - h \frac{\partial H(\mathbf{q}_n, \mathbf{p}_{n+1})}{\partial \mathbf{q}_n}, \quad (9)$$

which is implicit in general but explicit for Hamiltonians of the form (5). The second approach is to construct symplectic implicit Runge-Kutta algorithms. For the differential equation (1), the s -stage Runge-Kutta method is defined by (e.g., Ralston & Rabinowitz 1978)

$$k_i = f(x_n + h \sum_{j=1}^s a_{ij} k_j), \quad x_{n+1} = x_n + h \sum_{i=1}^s b_i k_i. \quad (10)$$

Runge-Kutta methods are symplectic if they satisfy a simple algebraic test (Sanz-Serna & Calvo 1994)

$$b_i a_{ij} + b_j a_{ji} - b_i b_j = 0, \quad 1 \leq i, j \leq s. \quad (11)$$

On setting $i = j$ in (11), it is evident that all symplectic Runge-Kutta methods are necessarily implicit. The best known examples are the Gauss-Legendre Runge-Kutta methods (e.g., Sanz-Serna & Calvo 1994). The simplest can be written

$$x_{n+1} = x_n + h f \left[\frac{1}{2}(x_n + x_{n+1}) \right], \quad (12)$$

which is the second-order implicit midpoint method. A symplectic fourth-order two-stage Runge-Kutta method is given by

$$a_{11} = a_{22} = \frac{1}{4}, \quad a_{12} = \frac{1}{4} - \frac{1}{6}\sqrt{3}, \quad a_{21} = \frac{1}{4} + \frac{1}{6}\sqrt{3}, \quad b_1 = b_2 = \frac{1}{2}. \quad (13)$$

More generally, the Gauss-Legendre Runge-Kutta method is the unique s -stage method with order $2s$, and this method is always symplectic. These attractive features are offset by the computational cost of solving the implicit equations (10).

A limitation of SIAs is that they are difficult to generalize to variable timesteps. When a standard variable timestep prescription is applied to an SIA, its performance is no better than that of non-symplectic integrators. The reason is simply that the mapping $G_{h(x)}(x)$ is usually not symplectic even when $G_h(x)$ is. This is a serious problem, since most applications benefit from a variable timestep. One way to introduce variable timestep is by extending the phase space (Mikkola 1997). Suppose we wish to use a timestep $g(\mathbf{q}, \mathbf{p})$. We define an extended phase space $(\mathbf{Q}, \mathbf{P}) = ((q_0, \mathbf{q}), (p_0, \mathbf{p}))$ by $q_0 = t$ and $p_0 = -E$, where t is time and E is energy. We then define a new Hamiltonian

$$\Gamma(\mathbf{Q}, \mathbf{P}) = g(\mathbf{q}, \mathbf{p}) [H(\mathbf{q}, \mathbf{p}) + p_0]. \quad (14)$$

The equations of motion for the Hamiltonian Γ in the extended phase space with fictitious time τ are the same as the equations of motion for the Hamiltonian H in the original phase space, supplemented by the condition $dt/d\tau = g(\mathbf{q}, \mathbf{p})$. We may now integrate the Hamiltonian Γ using an SIA with fixed timestep $\Delta\tau = 1$, which corresponds to $\Delta t \simeq g$. A limitation of this approach is that the Hamiltonian Γ is generally not separable, so that leapfrog and its generalizations cannot be applied.

1.2. Reversible integration algorithms

Several well-known one-step second-order algorithms for the differential equation (1) are RIAs: for example, the implicit midpoint method (eq. 12), the trapezoidal method,

$$x_{n+1} = x_n + \frac{1}{2}h [f(x_n) + f(x_{n+1})], \quad (15)$$

and the explicit midpoint method,

$$x_{n+2} = x_n + hf(x_{n+1}). \quad (16)$$

Some SIAs are also RIAs when they are applied to reversible Hamiltonians. Leapfrog and its generalizations are reversible. A reversible version of leapfrog with variable timestep $g(\mathbf{q}, \mathbf{p})$ is given by (Huang & Leimkuhler 1997; Calvo et al. 1998)

$$\begin{aligned} \mathbf{q}' &= \mathbf{q}_n + \frac{h}{2\rho_n} \mathbf{p}_n, & \mathbf{p}' &= \mathbf{p}_n + \frac{h}{2\rho_n} \nabla U(\mathbf{q}'), \\ \rho_{n+1} &= \frac{2}{g(\mathbf{q}', \mathbf{p}')} - \rho_n, & \mathbf{p}_{n+1} &= \mathbf{p}' + \frac{h}{2\rho_{n+1}} \nabla U(\mathbf{q}'), \\ \mathbf{q}_{n+1} &= \mathbf{q}' + \frac{h}{2\rho_{n+1}} \mathbf{p}_{n+1}, & t_{n+1} &= t_n + \frac{h}{2} (\rho_n^{-1} + \rho_{n+1}^{-1}). \end{aligned} \quad (17)$$

Quinn et al. (1997) describe a closely related algorithm based on a discrete set of timesteps that depend only on \mathbf{p} or \mathbf{q} and are separated by factors of two.

A different approach to constructing RIAs is to modify non-reversible integration algorithms. For example, the following two operators are reversible even if \tilde{G}_h is not:

$$\tilde{G}_{h/2}T\tilde{G}_{h/2}^{-1}T, \quad (1 + T\tilde{G}_hT)^{-1}(1 + \tilde{G}_h); \quad (18)$$

if we write $\tilde{G}_h = 1 + hA + O(h^2)$ then both of these operators are equal to $1 + \frac{1}{2}h(A - TAT)$ to first order in h . Hut et al. (1997) describe numerical experiments with the second of these operators, calling it a “time-symmetrization meta-algorithm” since it can be applied to any one-step numerical integration algorithm. Reversible algorithms remain reversible with a variable timestep so long as the timestep is determined symmetrically by the location of the system at the start and end of the step, e.g. $h = \frac{1}{2}[g(x_n) + g(x_{n+1})]$ (Hut et al. 1995).

Special second-order differential equations of the form

$$\frac{d^2x}{dt^2} = F(x) \quad (19)$$

are reversible, and so can profitably be integrated using RIAs. A useful source of high-order RIAs is linear multistep methods (e.g., Henrici 1962; Gear 1971; Lambert 1973), which have the form

$$\sum_{j=0}^k (a_{k-j}x_{n-j} - h^2 b_{k-j}F_j) = 0, \quad (20)$$

where $x_j = x(t_0 + jh)$, $F_j = F(x_j)$. We may assume without loss of generality that $a_k = 1$. The method is explicit if $b_k = 0$ and otherwise implicit. Linear multisteps include the classic Störmer (explicit) and Cowell (implicit) methods, which are characterized by $a_k = 1$, $a_{k-1} = -2$, $a_{k-2} = 1$, and $a_{k-j} = 0$ for $j > 2$. It is easy to show that the requirement for reversibility is that $a_j = ca_{k-j}$ and $b_j = cb_{k-j}$ where $c = \pm 1$; thus the Störmer and Cowell methods are generally not reversible. Multistep RIAs are discussed by Lambert & Watson (1976), Quinlan & Tremaine (1990), and Fukushima (1998, 1999). In general, their performance over long time intervals on reversible dynamical systems is much better than Störmer-Cowell methods, although for occasional unfortunate choices of timestep their performance is ruined by timestep resonances (Quinlan 1999).

Systems of first-order differential equations such as (1) can be integrated by linear multistep methods of the form

$$\sum_{j=0}^k (\alpha_{k-j}x_{n-j} - h\beta_{k-j}f_{n-j}) = 0, \quad (21)$$

where $x_j = x(t_0 + jh)$, $f_j = f(x_j)$. We can assume without loss of generality that $\alpha_k = 1$; explicit methods have $\beta_k = 0$. These include the classic Adams-Basforth (explicit) and Adams-Moulton (implicit) methods, which have $\alpha_{k-1} = -1$ and $\alpha_{k-j} = 0$ for $j > 2$ (e.g., Henrici 1962; Gear 1971). Multistep methods for first-order differential equations are more general than multistep methods for special second-order equations, since any second-order equation can be written as a set of first-order equations. Moreover, implementing variable timesteps is easy in first-order equations – if we wish to use a timestep $g(x)$ we introduce a fictitious time τ by the relation $dt = g(x)d\tau$, and equation (1) can be rewritten as

$$\frac{dx}{d\tau} = g(x)f(x), \quad (22)$$

which can be integrated using unit timestep in τ .

The aim of this paper is to investigate linear multistep RIAs for first-order differential equations. An important earlier investigation is that of Cano & Sanz-Serna (1998), who found that such methods typically possess grave numerical instabilities. We review general linear multistep methods in §2, multistep RIAs in §2.1, together with their instabilities in §2.2. We show in §3 that it is possible to construct some linear multistep RIAs that are not subject to the Cano & Sanz-Serna instabilities. A general discussion of stable multistep RIAs with up to 6 steps is given in §3.1 – §3.3. Finally, §4 describes numerical examples based on integrating Kepler orbits and §5 discusses our results.

2. Linear multistep methods

Following Henrici (1962) and Lambert (1973), we associate with (21) the linear operator

$$L[x(t), h] = \sum_{j=0}^k \{\alpha_{k-j}x[t + (k-j)h] - h\beta_{k-j}x'[t + (k-j)h]\}. \quad (23)$$

We can expand $x(t)$ in a Taylor series to obtain

$$L[x(t), h] = \sum_{q=0}^{\infty} C_q h^q x^{(q)}(t), \quad (24)$$

where

$$C_0 = \sum_{l=0}^k \alpha_l, \quad C_q = \frac{1}{q!} \sum_{l=0}^k \alpha_l l^q - \frac{1}{(q-1)!} \sum_{l=0}^k \beta_l l^{q-1}, \quad q = 1, 2, \dots \quad (25)$$

The order p of the multistep is the unique integer for which $C_0 = \dots = C_p = 0$, $C_{p+1} \neq 0$. The constant $C = C_{p+1}/\sigma(1)$ is known as the error constant and is a measure of the local

truncation error. Now define the characteristic polynomials

$$\rho(\xi) = \sum_{j=0}^k \alpha_j \xi^j, \quad \sigma(\xi) = \sum_{j=0}^k \beta_j \xi^j. \quad (26)$$

If $x(t) = \exp(\lambda t)$, then

$$L[x(t), h] = e^{\lambda t} [\rho(e^{\lambda h}) - \lambda h \sigma(e^{\lambda h})], \quad (27)$$

which together with equation (24) implies

$$\rho(1+z) - \log(1+z) \sigma(1+z) = C_{p+1} z^{p+1} + O(z^{p+2}), \quad (28)$$

where p is the order and $z = \exp(\lambda h) - 1$. Order ≥ 0 requires

$$\rho(1) = \sum_{j=0}^k \alpha_j = 0, \quad (29)$$

and order ≥ 1 requires

$$\rho'(1) = \sigma(1). \quad (30)$$

A multistep method is zero-stable if and only if the roots of $\rho(\xi)$ lie inside the unit circle in the complex plane, or are on the unit circle and simple (proofs of this are given by Henrici 1962, Gear 1971 and Lambert 1973). Zero-stability ensures that the parasitic solutions generated by the additional roots of the difference equation (which is of order k , while the original differential equation (1) has order one) do not grow, at least in the limit of zero timestep. We will discuss other forms of stability shortly in §2.2.

We assume that the polynomials $\rho(\xi)$ and $\sigma(\xi)$ have no common roots other than 1, for the following reason. Suppose that $\xi_0 \neq 1$ is a common root, so that $(\xi - \xi_0)$ is a common factor. Then $\rho(\xi) = (\xi - \xi_0)\tilde{\rho}(\xi)$, $\sigma(\xi) = (\xi - \xi_0)\tilde{\sigma}(\xi)$ where $\tilde{\rho}(\xi)$ and $\tilde{\sigma}(\xi)$ are polynomials of degree $k-1$. Then equation (28) may be written

$$\tilde{\rho}(1+z) - \log(1+z) \tilde{\sigma}(1+z) = \frac{C_{p+1}}{1-\xi_0} z^{p+1} + O(z^{p+2}). \quad (31)$$

Thus $\tilde{\rho}(\xi), \tilde{\sigma}(\xi)$ define a $(k-1)$ -step method with the same order and the same error constant ($C = C_{p+1}/\sigma(1) = C_{p+1}/[(1-\xi_0)\tilde{\sigma}(1)]$) as the original k -step method, and there is no obvious reason why the simpler method should not be used instead.

There are $2k+1$ unknown coefficients in equation (21) (since $\alpha_k = 1$), and therefore in principle these coefficients can be chosen so that the order is $2k$ (or $2k-1$ if the method is explicit, with $\beta_k = 0$). However, the maximum order of a zero-stable multistep method is $k+1$ if k is odd and $k+2$ if k is even (Henrici 1962).

2.1. Reversible multistep methods

Suppose that a trajectory $\{x_{n-k}, x_{n-k+1}, \dots, x_n\}$, $\{f_{n-k}, f_{n-k+1}, \dots, f_n\}$ satisfies the difference equation (21). The same segment of the time-reversed trajectory is given by $\{Tx_n, Tx_{n-1}, \dots, Tx_{n-k}\}$, $\{g_n, g_{n-1}, \dots, g_{n-k}\}$, where T is the time-reversal operator and $g_k = f(Tx_k)$. We shall assume that $x_k = (\mathbf{r}_k, \mathbf{v}_k)$ and that $f_k = (\mathbf{v}_k, -\nabla\Phi(\mathbf{r}_k))$. Then $T = \text{diag}(1, -1)$ and $f(Tx) = -Tf(x)$. In an RIA the time-reversed trajectory should also satisfy the difference equation (21), that is

$$\sum_{j=0}^k (\alpha_{k-j} Tx_{n-k+j} - h\beta_{k-j} g_{n-k+j}) = 0. \quad (32)$$

Since $g_j = f(Tx_j) = -Tf_j$, we may operate with T to obtain

$$\sum_{j=0}^k (\alpha_{k-j} x_{n-k+j} + h\beta_{k-j} f_{n-k+j}) = 0, \quad (33)$$

or, equivalently,

$$\sum_{j=0}^k (\alpha_j x_{n-j} + h\beta_j f_{n-j}) = 0. \quad (34)$$

If (34) is to be satisfied whenever (21) is satisfied, then we must have

$$\alpha_{k-j} = c\alpha_j, \quad \beta_{k-j} = -c\beta_j, \quad (35)$$

where c is a constant. Applying this relation twice gives $c^2 = 1$ so $c = \pm 1$. If $c = +1$, we shall say that the multistep method has even parity; if $c = -1$, the parity is odd. The characteristic polynomials (26) now satisfy

$$\rho(\xi) = c\xi^k \rho(\xi^{-1}), \quad \sigma(\xi) = -c\xi^k \sigma(\xi^{-1}). \quad (36)$$

Now let $\xi_j, j = 1, \dots, k$ be the roots of $\rho(\xi)$. Equation (36) implies that if ξ_j is a root then so is ξ_j^{-1} . For zero-stability, the roots cannot lie outside the unit circle – therefore they must lie on the unit circle, and moreover they must be simple. Equation (29) guarantees that $\xi_1 = 1$ is a root for any method with order ≥ 0 . This root is simple if $\rho'(1) \neq 0$, and equation (30) then requires that $\sigma(1) \neq 0$ for any method with order ≥ 1 . However, even-parity methods have $\sigma(1) = \sum_{j=0}^k \beta_j = 0$. Therefore, even-parity methods are not zero-stable and we can restrict our attention to odd-parity methods, $c = -1$.

If the reversibility criterion (35) is satisfied, then

$$L[x(t), h] = cL[x(t + kh), -h]. \quad (37)$$

Using (24) and the Taylor series expansion for $x(t + kh)$, we may derive the constraint

$$C_p = c \sum_{n=0}^p \frac{(-1)^{p-n} k^n}{n!} C_{p-n}. \quad (38)$$

We can re-write this equation as

$$C_p [1 - c(-1)^p] = \sum_{n=1}^p \frac{(-1)^{p-n} k^n}{n!} C_{p-n}. \quad (39)$$

If $c(-1)^p = -1$, then this equation implies that $C_p = 0$ if $C_0 = \dots = C_{p-1} = 0$ and thus the order cannot be $p - 1$. Therefore, odd-parity methods have even order.

The stability of multistep methods for oscillatory problems can be parametrized by the interval of periodicity introduced by Lambert & Watson (1976). Suppose the right-hand side of equation (1) is $f(x, t) = i\omega x$, with ω real. Then, the multistep method (21) becomes a linear difference equation, with solution $x_n = a\xi^n$. Here, a and ξ are complex constants, the latter satisfying

$$\rho(\xi) - i\omega h \sigma(\xi) = 0 \quad \text{or} \quad g(\theta) \equiv -i \frac{\rho(e^{i\theta})}{\sigma(e^{i\theta})} = \omega h. \quad (40)$$

The interval of periodicity is the largest value of ωh such that all of the roots of the first of equations (40) lie on the unit circle. Outside the interval of periodicity, the solution grows exponentially and hence is unstable. For reversible methods with odd parity, we may write

$$g(\theta) = \frac{\sum_{j=0}^k \alpha_j \sin[(j - \frac{1}{2}k)\theta]}{\sum_{j=0}^k \beta_j \cos[(j - \frac{1}{2}k)\theta]}. \quad (41)$$

If the multistep method is zero-stable, then $\rho(\xi)$ has k distinct roots on the unit circle. Thus, $g(\theta)$ has k distinct roots on the interval $[-\pi, \pi]$. For sufficiently small values of ωh , the equation $g(\theta) = \omega h$ will still have k roots. As ωh is increased, eventually a pair of these roots will disappear. This occurs at the smallest local maximum of $g(\theta)$ and marks the end of the interval of periodicity. So, a plot of $g(\theta)$ can be used to determine the interval of periodicity (Fukushima 1998).

2.2. Instabilities in reversible multisteps

The growth of errors in multistep methods is discussed by Henrici (1962), Gear (1971) and especially by Cano & Sanz-Serna (1998). For our purposes, a limited heuristic version

of these analyses is sufficient. Let $\{x_j\}$ be a solution of the multistep method (21). Now perturb the solution to $\{x_j + e_j\}$, $|e_j| \ll |x_j|$. Linearizing equation (21), we have

$$\sum_{j=0}^k (\alpha_{k-j} - h\beta_{k-j} f'_{n-j}) e_{n-j} = 0, \quad (42)$$

where $f'_j = \partial f(x_j)/\partial x$. Now look for solutions of the form $e_n = \xi^n y(t_0 + nh)$ where $y(t)$ is smooth and ξ is a complex constant. In the limit $h \rightarrow 0$, $x_n \rightarrow \tilde{x}(t_0 + nh)$, where $\tilde{x}(t)$ is the accurate solution of the differential equation (1) and therefore is smooth. Then (42) becomes

$$\sum_{j=0}^k \left[\alpha_j - h\beta_j \frac{\partial f}{\partial x}(\tilde{x}(t + jh)) \right] \xi^j y(t + jh) = 0, \quad (43)$$

where $t = t_0 + (n-k)h$. Now expand in a Taylor series in h . To order h^0 we have $y(t)\rho(\xi) = 0$, which requires that ξ is one of the roots $\xi_j, j = 1, \dots, k$ of the polynomial ρ . To order h we have

$$\frac{dy(t)}{dt} = \left(\frac{\sum_{j=0}^k \beta_j \xi^j}{\sum_{j=0}^k j \alpha_j \xi^j} \right) y(t) \frac{\partial f}{\partial x}(\tilde{x}(t)) = \left[\frac{\sigma(\xi)}{\xi \rho'(\xi)} \right] \frac{\partial f}{\partial x}(\tilde{x}(t)). \quad (44)$$

Thus, as $h \rightarrow 0$, the linearized difference equation (42) has solutions of the form

$$e_n = \sum_{j=1}^k a_j \xi_j^n y_j(t_0 + nh), \quad (45)$$

where $y_j(t)$ satisfies the differential equation

$$\frac{dy_j}{dt} = \lambda_j \frac{\partial f(\tilde{x}(t))}{\partial x} y_j(t), \quad (46)$$

and the growth parameters are

$$\lambda_j = \frac{\sigma(\xi_j)}{\xi_j \rho'(\xi_j)}, \quad j = 1, \dots, k. \quad (47)$$

This should be contrasted with the variational equation of the orbit itself. If the trajectory $\tilde{x}(t)$ is perturbed to $\tilde{x}(t) + \tilde{e}(t)$, $|\tilde{e}| \ll |\tilde{x}|$, then

$$\frac{d\tilde{e}(t)}{dt} = \frac{\partial f(\tilde{x}(t))}{\partial x} \tilde{e}(t). \quad (48)$$

Cano & Sanz-Serna (1998) point out that the variational equations (46) and (48) generally have quite different solutions, and hence the former can be unstable even if the latter is stable. However, this instability can be evaded for special values of the growth parameters λ_j : for $\lambda_j = 1$, equations (47) and (48) are the same, for $\lambda_j = -1$, equation (47) is simply

the time-reversed version of equation (48), and for $\lambda_j = 0$, the solution of equation (47) is simply $y_j = \text{const}$. We use the term “zero-growth” methods to denote multistep methods such that $\lambda_j \in \{-1, 0, 1\}$, $j = 1, \dots, k$. Cano (1996) has shown that for the reversible planar Kepler problem, these are the only possible choices for the growth parameters λ_j to ensure stability, although for other potentials this may not be the case.

Multistep methods for integrating the special second-order equation $x'' = f(x, t)$ (Lambert & Watson 1976; Quinlan & Tremaine 1990) are not generally subject to this sort of instability, for the following reason. The expansion of the analog to equation (43) in this case yields $y(t)\rho(\xi) = 0$ to order h^0 and $y'(t)\rho'(\xi) = 0$ to order h . Satisfying these two equations simultaneously requires that ξ is a double root of $\rho(\xi)$; therefore there is no instability if all of the roots of $\rho(\xi)$ are simple (Cano & Sanz-Serna 1998).

3. Zero-growth methods

In this section, all the zero-growth multistep algorithms with up to six steps are found. Let us begin with some general results for stable, odd-parity, multistep RIAs, specified by the characteristic polynomials $\rho(\xi)$ and $\sigma(\xi)$. Let ξ_j , $j = 1, \dots, k$ be the roots of $\rho(\xi)$; for zero-stable reversible methods, these are distinct, lie on the unit circle and are either real (+1 or -1) or appear in complex-conjugate pairs. Equation (29) implies that 1 is always a root, which we denote ξ_1 . Therefore, -1 is also a root if and only if the total number of roots k is even; when present, we denote this root as ξ_2 . We normalize the multistep method so that $\alpha_k = 1$ and

$$\rho(\xi) = \prod_{j=1}^k (\xi - \xi_j). \quad (49)$$

We now demand that the growth parameter associated with the root ξ_l is $\lambda_l \in \{-1, 0, 1\}$ (note that $\lambda_1 = +1$ by eq. 30). From equation (47), this requires that

$$\sigma(\xi_l) = \lambda_l \xi_l \rho'(\xi_l) = \lambda_l \xi_l \prod_{j \neq l} (\xi_l - \xi_j). \quad (50)$$

The unique polynomial of order k that passes through the points (50) and satisfies the symmetry condition (36) is

$$\sigma(\xi) = \frac{1}{2} \sum_{l=1}^k \lambda_l (\xi + \xi_l) \prod_{j \neq l} (\xi - \xi_j), \quad (51)$$

with $\lambda_j = \lambda_l$ when $\xi_j \xi_l = 1$. An alternative form is

$$\sigma(\xi) = \frac{1}{2} \rho(\xi) \sum_{l=1}^k \lambda_l \frac{\xi + \xi_l}{\xi - \xi_l}. \quad (52)$$

Note that if $\lambda_l = 0$ then ξ_l is a root of both $\rho(\xi)$ and $\sigma(\xi)$. In this case, there is a zero-growth multistep RIA with the same order and error constant but fewer steps (see §2). Therefore, we restrict our attention to methods with $\lambda_l \in \{-1, 1\}$.

The method is explicit if $\sigma(0) = 0$, which in turn requires

$$\sum_{j=1}^k \lambda_j = 0, \quad (53)$$

a condition that can only be satisfied if k is even.

A k -step method is completely specified by the k^{th} -order polynomials $\rho(\xi)$, $\sigma(\xi)$. In a stable multistep RIA with k even, the roots of $\rho(\xi)$ are $+1$, -1 , $x_j \pm iy_j$ where $x_j^2 + y_j^2 = 1$, $j = 1, \dots, \frac{1}{2}(k-2)$. For k odd, the root at -1 is not present and the index runs to $\frac{1}{2}(k-1)$. In a zero-growth method, the polynomial $\sigma(\xi)$ is determined by equation (51) once $\rho(\xi)$ and the signs λ_j are specified. We now discuss all stable, zero-growth, multistep RIAs of ≤ 6 steps. We label the interesting methods by $\text{SZ}kp$ where k is the number of steps and “p” is an optional suffix that distinguishes different methods with the same k .

3.1. One- and two-step methods

Since $\xi_1 = 1$ is always a root, for $k = 1$ we must have $\rho(\xi) = \xi - 1$. Since $\lambda_1 = +1$ by equation (30), the zero-growth requirement is automatically satisfied. Equation (51) requires that $\sigma(\xi) = \frac{1}{2}(\xi + 1)$, which yields the trapezoidal method (eq. 15)

$$x_{n+1} = x_n + \frac{1}{2}h(f_{n+1} + f_n); \quad \text{method SZ1} \quad (54)$$

The first few terms of the Taylor series (24) are

$$C_0 = 0, \quad C_1 = 0, \quad C_2 = 0, \quad C_3 = -\frac{1}{12}; \quad (55)$$

thus the error constant is $C = -\frac{1}{12}$ and the method is second-order. The function $g(\theta)$ (eq. 40) is $2 \tan \frac{1}{2}\theta$, so the interval of periodicity is infinite.

For $k = 2$ the roots of $\rho(\xi)$ can only be ± 1 ($\xi_1 = 1$ is always a root; ξ_2 must be real since ξ_2^* is also a root and there are only two roots; ξ_2 must be on the unit circle and distinct from ξ_1 ; thus $\xi_2 = -1$). Thus, the first characteristic polynomial is

$$\rho(\xi) = \xi^2 - 1. \quad (56)$$

There are two choices for the second characteristic polynomial $\sigma(\xi)$, depending on $\lambda_2 \in \{-1, 1\}$:

$$\sigma(\xi) = 2\xi, \quad \text{or} \quad \sigma(\xi) = \xi^2 + 1. \quad (57)$$

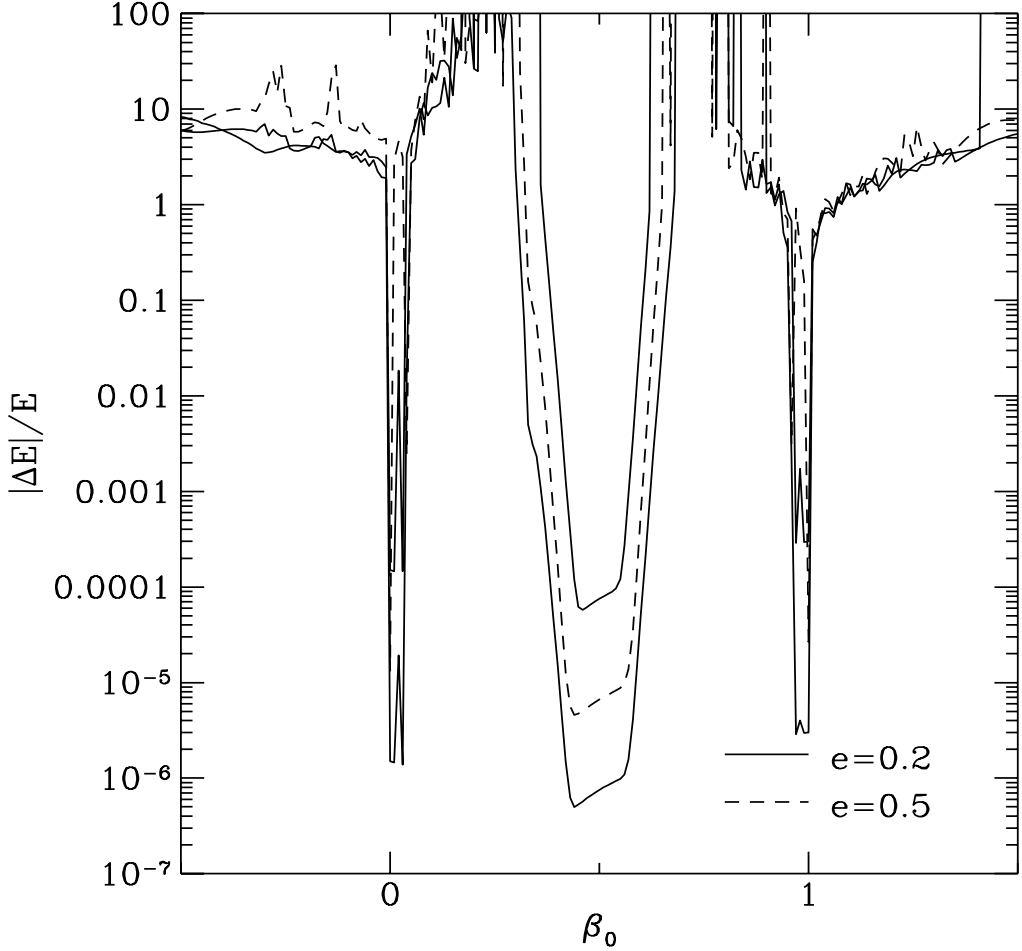


Fig. 1.— The fractional energy error after integrating the standard Kepler problem ($a = 1$, $GM = 1$) for 100 time units using the 2-step RIA (61), as a function of the parameter β_0 . The two solid curves were computed with timesteps $h = 0.01$ and 0.001 for eccentricity $e = 0.2$, while the dashed curve has $h = 0.001$ and $e = 0.5$. Off-scale energy errors indicate that an implicit timestep did not converge after 20 iterations. The minima at $\beta_0 = 0, \frac{1}{2}, 1$ correspond to the explicit midpoint method, the trapezoidal method, and the trapezoidal method with a timestep of $2h$.

The first of these gives the explicit midpoint method (eq. 16),

$$x_{n+1} = x_{n-1} + 2hf_n \quad \text{method SZ2.} \quad (58)$$

The first few terms of the Taylor series (24) are

$$C_0 = 0, \quad C_1 = 0, \quad C_2 = 0, \quad C_3 = \frac{1}{3}; \quad (59)$$

thus the error constant is $C = \frac{1}{6}$ and the method is second-order. The function $g(\theta)$ is $\sin \theta$ so the interval of periodicity is $(\omega h)_{\max} = 1$. The second equation for $\sigma(\xi)$ in (57) yields

$$x_{n+1} = x_{n-1} + h(f_{n+1} + f_{n-1}), \quad (60)$$

which is the same as the trapezoidal method (54), with a timestep of $2h$.

All of these two-step methods are special cases of a one-parameter family of multistep RIAS,

$$x_{n+1} = x_{n-1} + h[\beta_0 f_{n+1} + 2(1 - \beta_0) f_n + \beta_0 f_{n-1}]. \quad (61)$$

The explicit midpoint method (eq. 58) has $\beta_0 = 0$ and the trapezoidal method with timestep $2h$ (eq. 60) has $\beta_0 = 1$. When $\beta_0 = \frac{1}{2}$, the method is simply the composition of two trapezoidal steps (eq. 54). Milne's method ($\beta_0 = \frac{1}{3}$) is the two-step method of maximum possible order ($p = 4$), but its disadvantage is that its growth parameter $\lambda_2 = -\frac{1}{3}$ and so it is susceptible to numerical instability. The interval of periodicity $(\omega h)_{\max} = (1 - 2\beta_0)^{-1/2}$ for $\beta_0 < \frac{1}{2}$ and infinity for $\beta_0 \geq \frac{1}{2}$. To compare these methods we have integrated a Kepler orbit with unit semimajor axis and period 2π for 100 time units using various eccentricities and timesteps (Fig. 1). Even for timesteps as low as $h = 0.001$, the relative energy error $|\Delta E|/E \gg 1$, except near the zero-growth methods at $\beta_0 = 0, \frac{1}{2}, 1$. In particular, the second-order zero-growth methods – even the explicit method at $\beta_0 = 0$ – exhibit much better behavior than the fourth-order Milne's method.

3.2. Three- and four-step methods

For $k = 3$, the distinct roots of ξ can only be $\xi_1 = 1$ and $\xi_{2,3} = u \pm iv$ where $|u| < 1$ and $v = (1 - u^2)^{1/2}$. Thus,

$$\rho(\xi) = \xi^3 - (2u + 1)\xi^2 + (2u + 1)\xi - 1. \quad (62)$$

There are two choices for $\sigma(\xi)$. The first choice is to take $\lambda_2 = \lambda_3 = +1$, so that we have

$$\sigma(\xi) = \frac{3}{2}\xi^3 - (\frac{1}{2} + u)\xi^2 - (\frac{1}{2} + u)\xi + \frac{3}{2}. \quad (63)$$

The first few terms of the Taylor series (24) are

$$C_0 = 0, \quad C_1 = 0, \quad C_2 = 0, \quad C_3 = -\frac{13}{6} + \frac{1}{6}u. \quad (64)$$

$C_3 = 0$ has no solution for $|u| < 1$ so the method is second-order; the interval of periodicity is infinite. The second choice is to take $\lambda_2 = \lambda_3 = -1$ so that we have

$$\sigma(\xi) = -\frac{1}{2}\xi^3 + (\frac{3}{2} - u)\xi^2 + (\frac{3}{2} - u)\xi - \frac{1}{2}. \quad (65)$$

The first few terms of the Taylor series (24) are

$$C_0 = 0, \quad C_1 = 0, \quad C_2 = 0, \quad C_3 = \frac{11}{6} + \frac{1}{6}u. \quad (66)$$

Once again, $C_3 = 0$ has no solution for $|u| < 1$ so the method is second-order. The interval of periodicity ranges from $2^{-1/2}$ as $u \rightarrow -1$ to 0 as $u \rightarrow 1$.

For $k = 4$, the distinct roots of ξ can only be $\xi_1 = 1$, $\xi_2 = -1$ and $\xi_{3,4} = u \pm iv$ where $|u| < 1$ and $v = (1 - u^2)^{1/2}$. Thus,

$$\rho(\xi) = \xi^4 - 2u\xi^3 + 2u\xi - 1. \quad (67)$$

There are four choices for $\sigma(\xi)$: $\lambda_2 \in \{-1, +1\}$, $\lambda_3 = \lambda_4 \in \{-1, +1\}$. None of these yield methods of order > 2 for $|u| < 1$.

The three- and four-step methods have no obvious advantage over the trapezoidal or explicit midpoint methods, and we will not explore them further.

3.3. Five- and six-step methods

For $k = 5$, the distinct roots of ξ are $\xi_1 = 1$, $\xi_{2,3} = u_1 \pm iv_1$ and $\xi_{4,5} = u_2 \pm iv_2$, where $|u_j| < 1$ and $v_j = (1 - u_j^2)^{1/2}$. There are three choices for $\sigma(\xi)$: $(\lambda_2, \lambda_4) = (-1, -1), (-1, +1)$, or $(+1, +1)$ (note that $(+1, -1)$ is not a distinct choice), with $\lambda_3 = \lambda_2$ and $\lambda_5 = \lambda_4$. The choices $(\lambda_2, \lambda_4) = (-1, -1), (+1, +1)$ yield only second-order methods. The choice $(\lambda_2, \lambda_4) = (-1, +1)$ yields a fourth-order method if

$$u_2 = \frac{1 + 11u_1}{13 - u_1}, \quad u_1 \in (-1, 1), \quad u_2 \in (-\frac{5}{7}, 1). \quad (68)$$

The integration formula is

$$\begin{aligned} x_{n+1} = & (x_n - x_{n-3})(1 + 2u_1 + 2u_2) - 2(x_{n-1} - x_{n-2})(1 + u_1 + u_2 + 2u_1u_2) + x_{n-4} \\ & + \frac{1}{2}h[f_{n+1} + (f_n + f_{n-3})(1 + 2u_1 - 6u_2) \\ & + 2(f_{n-1} + f_{n-2})(1 - 3u_1 + u_2 + 2u_1u_2) + f_{n-4}] \end{aligned} \quad \text{method SZ5.} \quad (69)$$

The error constant is

$$C = \frac{C_5}{\sigma(1)} = \frac{17u_1 + 103}{1440(u_1 - 1)}. \quad (70)$$

For $k = 6$, the distinct roots of ξ are $\xi_1 = 1$, $\xi_2 = -1$, $\xi_{3,4} = u_1 \pm iv_1$ and $\xi_{5,6} = u_2 \pm iv_2$, where $|u_j| < 1$ and $v_j = (1 - u_j^2)^{1/2}$. There are six choices for $\sigma(\xi)$: $\lambda_2 = -1$ or $+1$ and $(\lambda_3, \lambda_5) = (-1, -1), (+1, -1), (+1, +1)$, with $\lambda_4 = \lambda_3$ and $\lambda_6 = \lambda_5$. The choices $(\lambda_3, \lambda_5) = (-1, -1)$ or $(+1, +1)$ yield only second-order methods. The choice $(\lambda_2, \lambda_3, \lambda_5) = (+1, +1, -1)$ yields a fourth-order method if

$$u_2 = \frac{1 + 2u_1}{4 - u_1}, \quad u_1 \in (-1, 1), \quad u_2 \in (-\frac{1}{5}, 1). \quad (71)$$

The error constant is

$$C = \frac{C_5}{\sigma(1)} = \frac{14 + u_1}{45(u_1 - 1)}. \quad (72)$$

The integration formula is

$$\begin{aligned} x_{n+1} = & 2(x_n - x_{n-4})(u_1 + u_2) - (x_{n-1} - x_{n-3})(1 + 4u_1u_2) + x_{n-5} \\ & + h[f_{n+1} + f_{n-5} - 4(f_n + f_{n-4})u_2 \\ & + (f_{n-1} + f_{n-3})(3 + 4u_1u_2) - 8f_{n-2}u_1] \end{aligned} \quad \text{method SZ6i,} \quad (73)$$

the label “i” stands for “implicit”.

The choice $(\lambda_2, \lambda_3, \lambda_5) = (-1, +1, -1)$ yields an explicit fourth-order method if

$$u_2 = \frac{7u_1 - 1}{u_1 + 5}, \quad u_1 \in (-\frac{1}{2}, 1), \quad u_2 \in (-1, 1). \quad (74)$$

The error constant is

$$C = \frac{C_5}{\sigma(1)} = \frac{19 + 11u_1}{180(1 - u_1)}. \quad (75)$$

The integration formula is

$$\begin{aligned} x_{n+1} = & 2(x_n - x_{n-4})(u_1 + u_2) - (x_{n-1} - x_{n-3})(1 + 4u_1u_2) + x_{n-5} \\ & + h[2(f_n + f_{n-4})(1 + u_1 - u_2) - 4(f_{n-1} + f_{n-3})(u_1 + u_2) + \\ & 4f_{n-2}(1 - u_1 + u_2 + 2u_1u_2)] \end{aligned} \quad \text{method SZ6e.} \quad (76)$$

The intervals of periodicity for the three fourth-order methods are shown in Figure 2. These are largest for u_1 near -1 and decrease rapidly for $u_1 > 0$. Thus, only methods with negative u_1 are of practical use. At best, the interval of periodicity is significantly smaller than that of comparable multistep RIAs for special second-order equations (Lambert & Watson 1976; Quinlan & Tremaine 1990; Fukushima 1998). This is the price of the greater generality of the present methods.

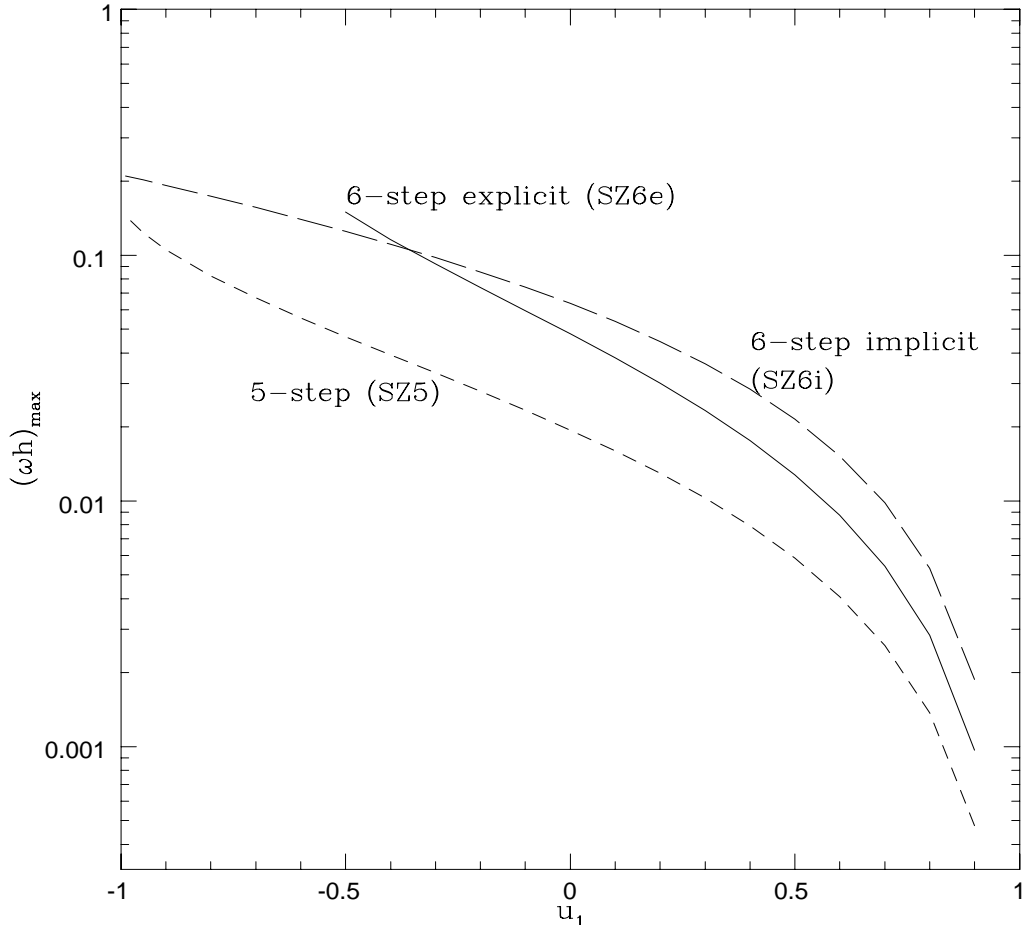


Fig. 2.— The interval of periodicity for three zero-growth, fourth-order RIAS: the five-step method SZ5 defined by equations (68) and (69), the 6-step implicit method SZ6i defined by (71) and (73), and the 6-step explicit method SZ6e defined by (74) and (76).

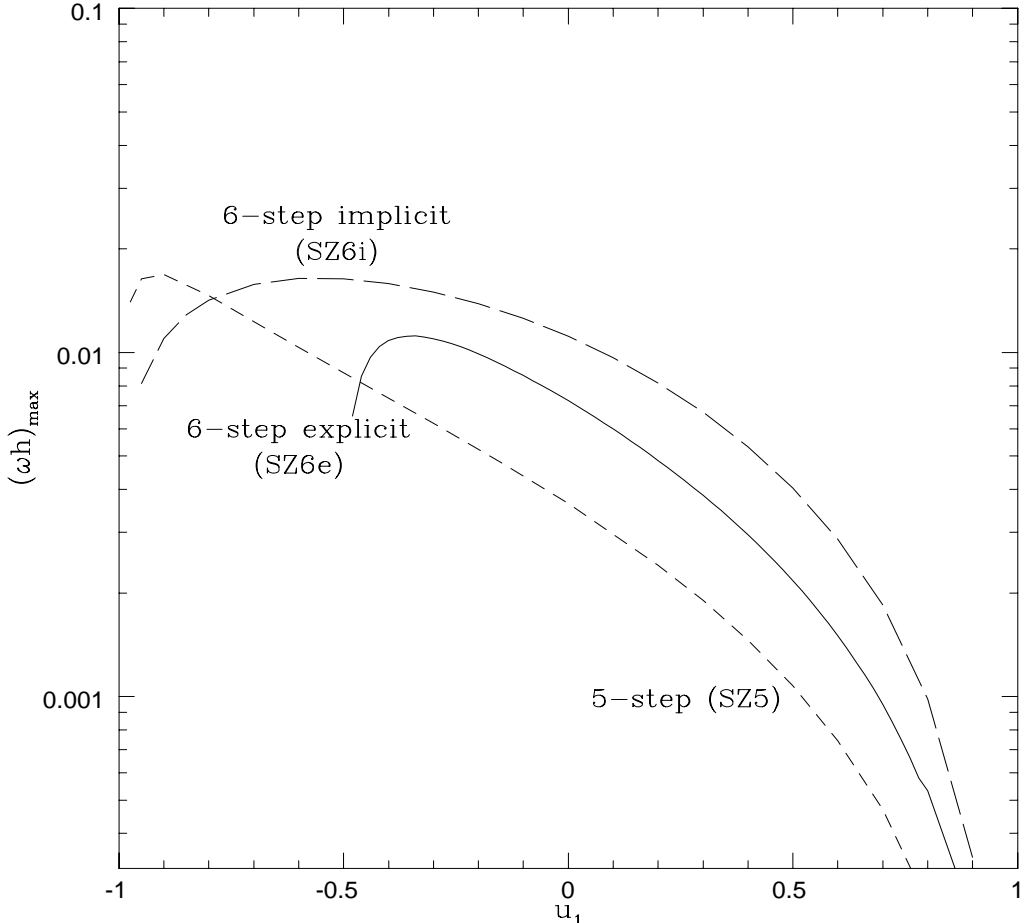


Fig. 3.— The largest timestep that can integrate a circular orbit in the reversible Kepler potential and maintain fractional energy error below 10^{-7} for 100 orbital periods. Results are shown for the three zero-growth, fourth-order RIAs: the five-step method SZ5 defined by equations (68) and (69), the 6-step implicit method SZ6i defined by (71) and (73), and the 6-step explicit method SZ6e defined by (74) and (76). Although results are displayed for circular orbits, the curves for mildly eccentric orbits ($e \lesssim 0.1$) are almost indistinguishable. This diagram can be compared with Figure 2, which shows the theoretical upper limit to the timestep for the harmonic oscillator potential.

4. Numerical experiments

This section supplements our theoretical analysis of multistep RIAs with numerical experiments using the Keplerian Hamiltonian $\frac{1}{2}v^2 - 1/r$. The equations of motion are

$$\frac{dx}{dt} = v_x, \quad \frac{dy}{dt} = v_y, \quad \frac{dv_x}{dt} = -\frac{x}{r^3}, \quad \frac{dv_y}{dt} = -\frac{y}{r^3}, \quad (77)$$

where $r^2 = x^2 + y^2$ and the gravitational constant G and the attracting mass M have been set to unity. Our test integrations follow an orbit with eccentricity e , unit semi-major axis, and orbital period 2π . The orbit is started at apocenter on the x -axis, so the initial conditions are

$$x = 1 + e, \quad y = 0, \quad v_x = 0, \quad v_y = [(1 - e)/(1 + e)]^{1/2}. \quad (78)$$

The interval of periodicity shown in Figure 2 gives the maximum stable timestep for the harmonic oscillator potential only. It is of greater relevance to astronomers to establish the timesteps that can be safely used to integrate circular or mildly eccentric orbits in the Kepler potential. Figure 3 shows the largest timestep for which the relative energy error is less than 10^{-7} after 100 orbital periods. The results displayed are for circular orbits, but the curves for mildly eccentric orbits ($e \lesssim 0.1$) are almost indistinguishable. A comparison between Figures 2 and 3 reveals that the timestep needed for accurate integration of Keplerian near-circular orbits is typically at least a factor of five smaller than would be naively inferred from the interval of periodicity.

Figure 4 shows a further test of the multistep RIAs. The standard Kepler problem is integrated for 100 time units with timestep $h = 0.003$ and eccentricities 0.2 and 0.5. A striking feature is that the error is almost independent of the parameter u_1 over a limited range, while outside this range the method is unstable. The stable range shrinks as the eccentricity increases. The dependence of energy error on timestep is explored in Figure 5. In this Figure, we have specialized to a single value of the parameter u_1 : -0.75 for SZ5 and SZ6i and -0.25 for SZ6e. All three methods display the expected dependence $\Delta E \propto h^4$ for $h < 0.01$. For larger values of h , the methods are unstable. We have also plotted the behavior of the classic fourth-order Adams-Bashforth (explicit) and Adams-Moulton (implicit) multistep methods. The classic methods exhibit similar errors for $h < 0.01$ but remain stable at much larger timesteps. The advantage of the reversible multistep methods only becomes clear over longer time intervals. Figure 6 shows that the maximum energy error in the reversible methods is constant at large times, while the energy error in the classical methods grows linearly.

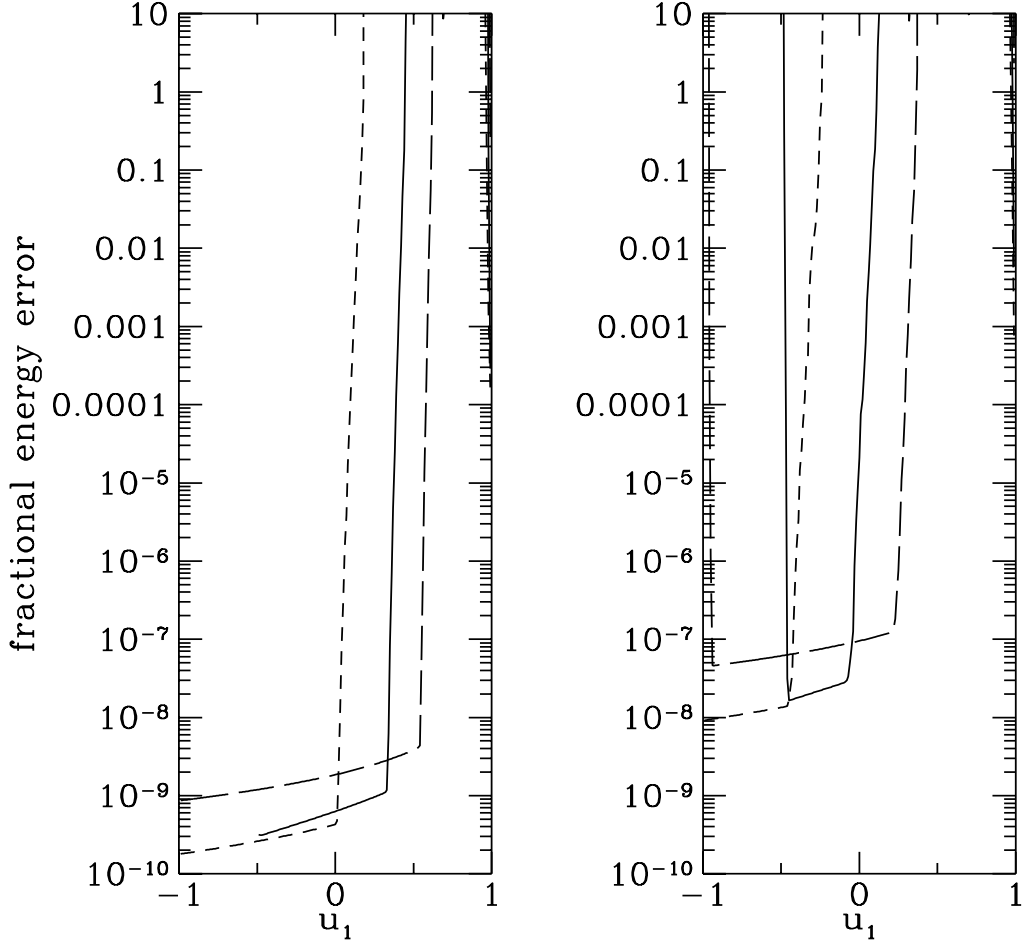


Fig. 4.— The fractional energy error after integrating the standard Kepler problem ($a = 1$, $GM = 1$) for 100 time units using timestep $h = 0.003$ and eccentricities 0.2 (left panel) and 0.5 (right panel). The figure shows results for three fourth-order methods: the five-step method SZ5 (short-dashed lines); the 6-step implicit method SZ6i (long-dashed lines), and the 6-step explicit method SZ6e (solid lines). The curves for $e = 0.5$ are always higher than the corresponding curves for $e = 0.2$.

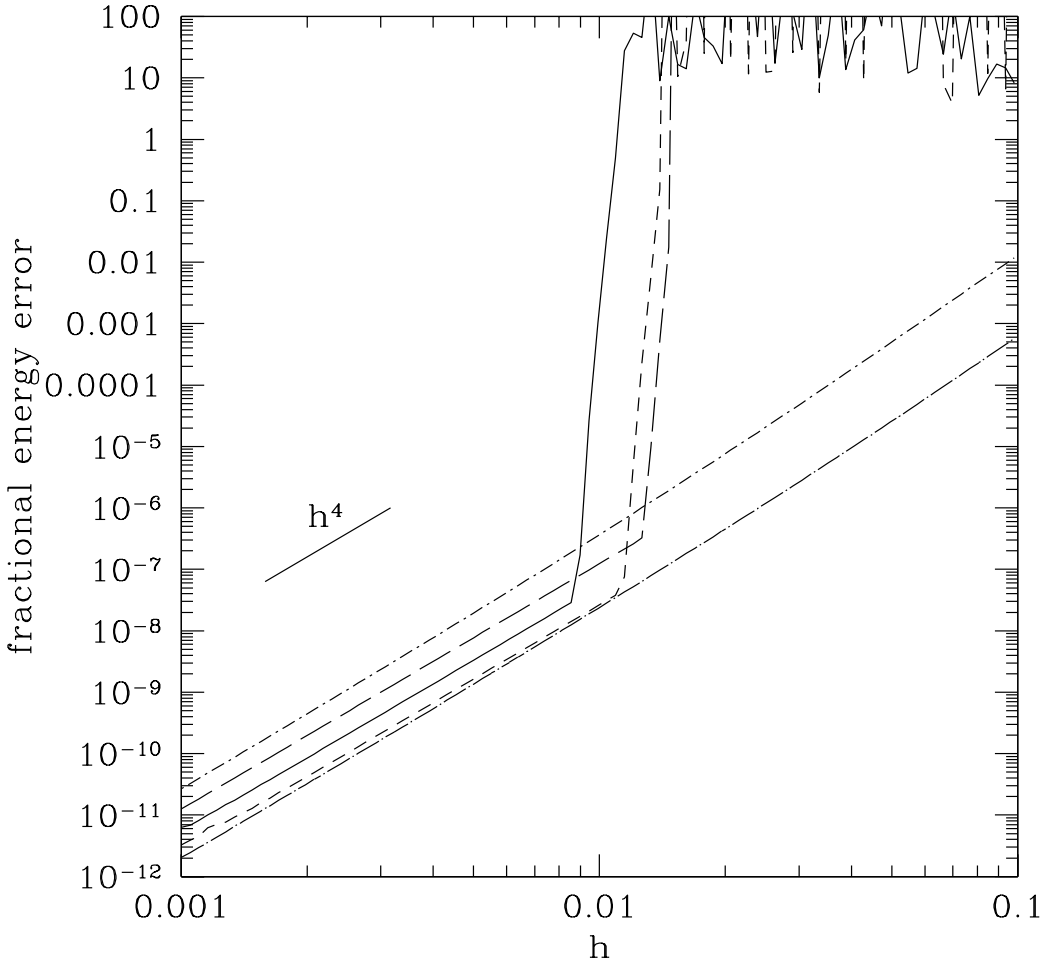


Fig. 5.— The fractional energy error after integrating the standard Kepler problem ($a = 1$, $GM = 1$) with eccentricity $e = 0.2$ for 100 time units. The figure shows results for three zero-growth, fourth-order RIAs: the five-step method SZ5 with $u_1 = -0.75$ (short-dashed line); the 6-step implicit method SZ6i with $u_1 = -0.75$ (long-dashed line); and the 6-step explicit method SZ6e with $u_1 = -0.25$ (solid line). Errors are also shown for two other fourth-order multistep methods: Adams-Basforth (dot-short dashed line) and Adams-Moulton (dot-long dashed line).

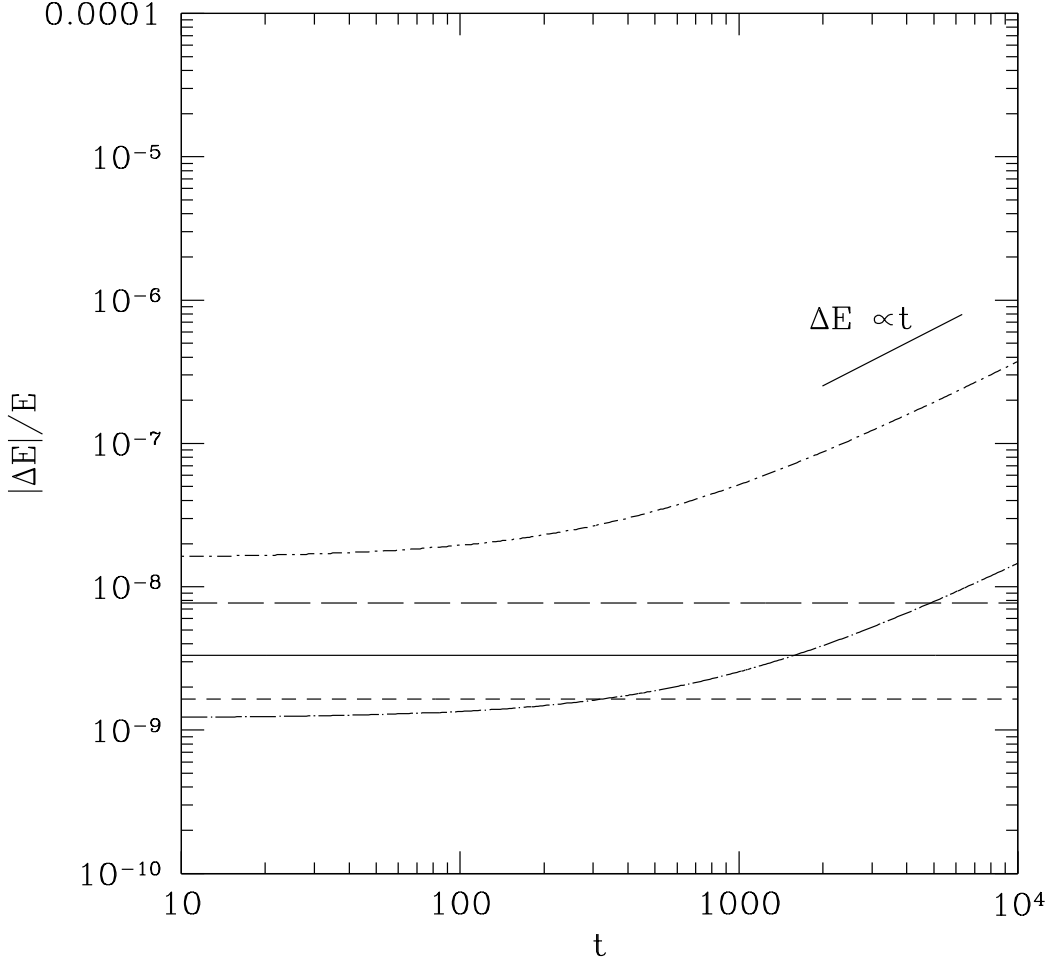


Fig. 6.— The maximum fractional energy error over integration time t for the standard Kepler problem ($a = 1$, $GM = 1$) with eccentricity $e = 0.2$ and timestep $h = 0.005$. The figure shows results for three zero-growth, fourth-order RIAS: the five-step method SZ5 with $u_1 = -0.75$ (short-dashed line); the 6-step implicit method SZ6i with $u_1 = -0.75$ (long-dashed line); and the 6-step explicit method SZ6e with $u_1 = -0.25$ (solid line). Errors are also shown for the fourth-order Adams-Basforth (dot-short dashed line) and Adams-Moulton methods (dot-long dashed line).

4.1. Variable timesteps

Variable timesteps are useful for eccentric Kepler orbits. To incorporate these, we introduce a fictitious time τ by the relation $dt = g(x, y)d\tau$, so the equations of motion become

$$\frac{dx}{d\tau} = g(x, y)v_x, \quad \frac{dy}{d\tau} = g(x, y)v_y, \quad \frac{dv_x}{d\tau} = -g(x, y)\frac{x}{r^3}, \quad \frac{dv_y}{d\tau} = -g(x, y)\frac{y}{r^3}, \quad \frac{dt}{d\tau} = g(x, y). \quad (79)$$

These are integrated using unit timestep in τ . We typically use $g(x, y) \propto r^{3/2}$ since this is the characteristic free-fall time from radius r . We parameterize the timestep by the number of force evaluations per unit time (or per radian, since the orbital period is 2π). This is distinct from the number of steps per radian because implicit methods require several iterations per step, and because some explicit methods – though not multistep methods – require several force evaluations per step. Figure 7 shows the fractional energy errors resulting from integrating Kepler orbits using the trapezoidal method (eq. 54, solid lines) and explicit adaptive leapfrog (eq. 17, dashed lines). Each step of the trapezoidal method was iterated to convergence, with the first approximation taken from the first-order Euler method – typically 3 iterations were required at the smallest timesteps, rising to ~ 10 at the largest. The energy errors are the maximum over 1000 time units or $500/\pi$ orbits. The results for shorter integrations over 100 time units are almost indistinguishable, showing that there is no secular energy drift with either integration method. Adaptive leapfrog generally gives energy errors that are smaller by about an order of magnitude, mostly because it is explicit so there are fewer force evaluations per timestep. We have conducted similar experiments with the explicit midpoint method (eq. 58, not shown in Figure) but this is much less successful at following high-eccentricity orbits, presumably because of its smaller interval of periodicity.

We next investigate the fourth-order multistep RIAs. These have relatively small intervals of periodicity and cannot reliably integrate high-eccentricity orbits. However, they are successful at following orbits with moderate eccentricities. Figure 8 shows the fractional energy errors resulting from integrating a Kepler orbit with eccentricity $e = 0.5$ using four methods: the explicit six-step method with $u_1 = -0.25$ (method SZ6e, eq. 76); the implicit six-step method with $u_1 = -0.75$ (method SZ6i, eq. 73); the implicit five-step method with $u_1 = -0.75$ (method SZ5, eq. 69). In all panels, the heavy solid line is the error resulting from integrating the eccentric orbit with variable timestep, the light solid line is the error from integrating the same orbit with fixed timestep, and the dashed line is the error from integrating a circular orbit with fixed timestep. For large timesteps, the implicit methods do not converge and in this case no energy error is plotted. For all four methods a variable timestep yields errors that are 1–2 orders of magnitude smaller than a fixed timestep (at the

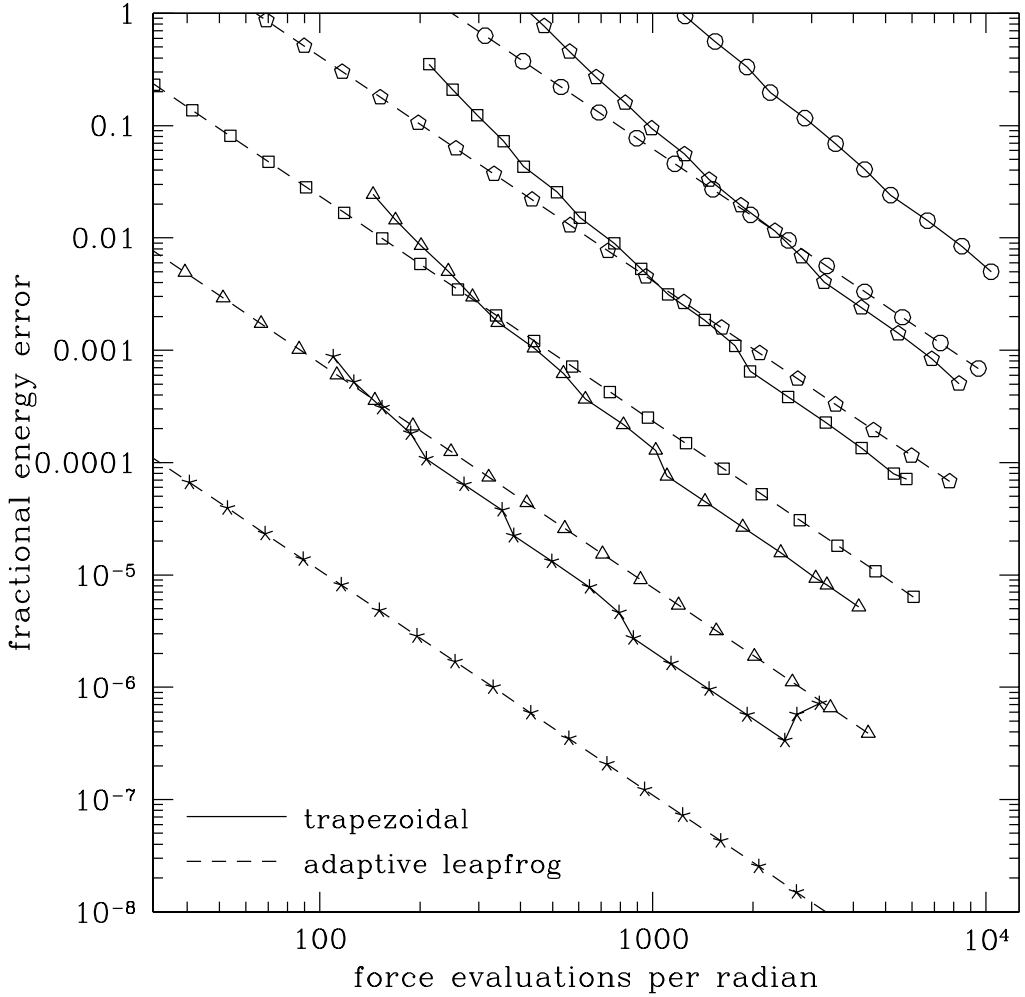


Fig. 7.— Results of integrating the differential equations for a Kepler orbit (79) for 1000 time units, using the trapezoidal method (eq. 54, solid lines) and explicit adaptive leapfrog (eq. 17, dashed lines). The orbit eccentricities are $e = 0.5$ (stars), 0.9 (triangles), 0.99 (squares), 0.999 (pentagons), 0.9999 (circles). The vertical axis is the maximum fractional energy error during the integration and the horizontal axis is the number of evaluations of the right-hand side of equations (79) per unit time (the orbital period is 2π).

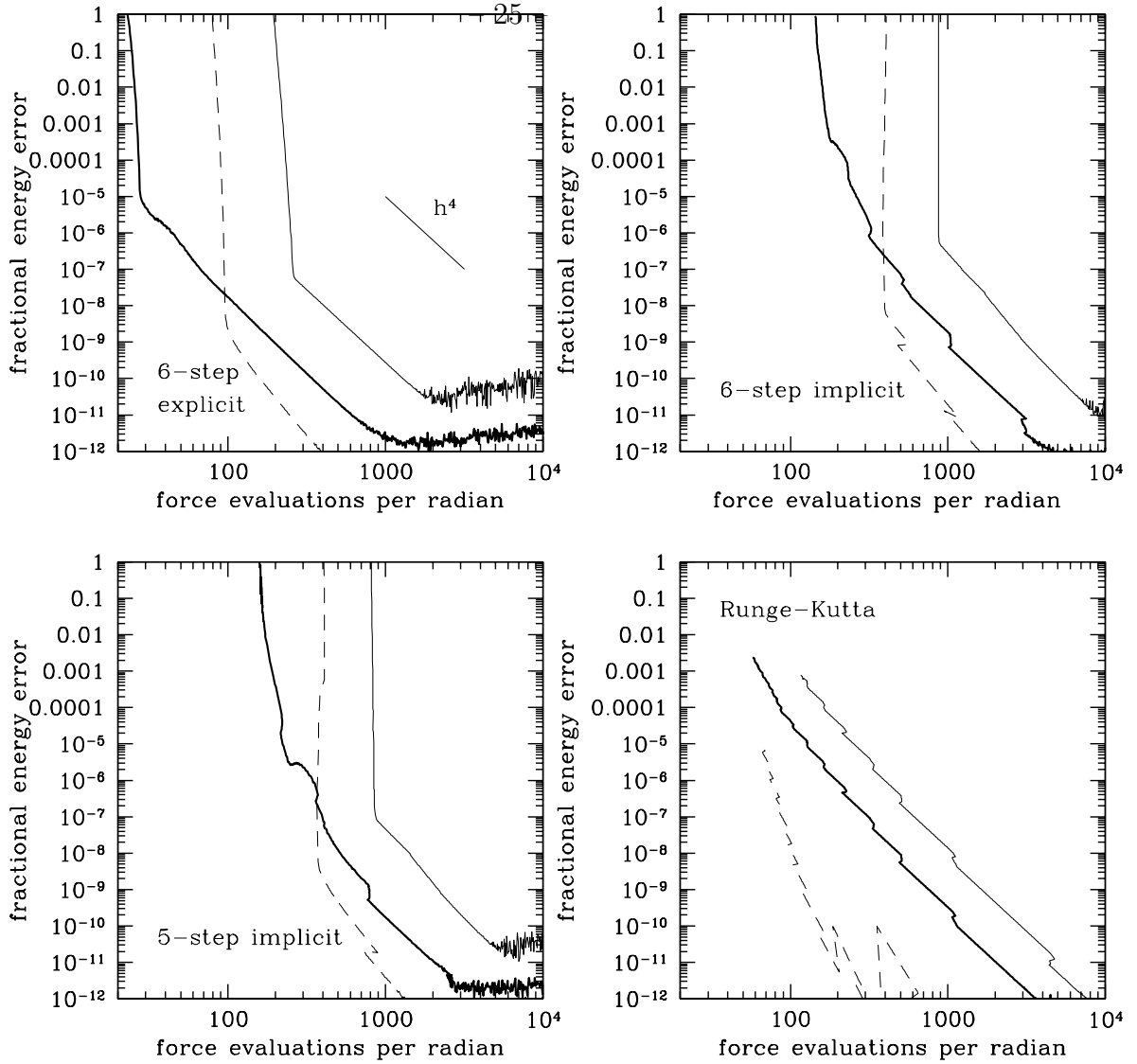


Fig. 8.— Integration of a Kepler orbit with eccentricity $e = 0.5$ by four fourth-order methods: the explicit six-step method with $u_1 = -0.25$ (method SZ6e, eq. 76); the implicit six-step method with $u_1 = -0.75$ (method SZ6i, eq. 73); the implicit five-step method with $u_1 = -0.75$ (method SZ5, eq. 69); and the implicit, fourth-order, two-stage Runge-Kutta RIA defined by equations (13). The heavy solid lines are the fractional energy errors for $e = 0.5$ and variable timestep, the light solid lines are for $e = 0.5$ and fixed timestep, and the dashed lines are for $e = 0$ and fixed timestep.

same number of function evaluations per unit time). The explicit multistep method performs much better than the implicit methods, in part because the implicit methods require 3–8 force evaluations per step to iterate to convergence. However, even if the convergence of the implicit multistep methods could be achieved in 2–3 iterations they would not perform significantly better than the explicit method on this test. A surprising result is that there is a range of the horizontal axis in which the multistep methods with variable timestep integrate eccentric orbits with smaller energy error than circular orbits.

4.2. Resonant instabilities

Toomre (1990, private communication) and Quinlan (1999) showed that multistep RIAs for the special second-order differential equation (19) suffer instabilities at unlucky timesteps at which there is a resonance between the oscillation frequencies of the solution and the method. This phenomenon must also occur in the multistep RIAs for first-order differential equations that are investigated here. Suppose the angular speed of the circular orbit given by the numerical method is ω . If the number of steps in the multistep RIA is at least 5 (or 6 for second-order differential equations), then there are two or more complex-conjugate pairs of roots of the characteristic polynomial (26) on the unit circle. These we write as $\xi_i = \exp(\pm i\theta_i)$ and $\xi_j = \exp(\pm i\theta_j)$. Quinlan (1999) shows that the troublesome timesteps h satisfy

$$\theta_i - \theta_j = 2\omega h. \quad (80)$$

In practice these resonant instabilities are never a concern for our zero-growth multistep RIAs. This is because the timesteps (80) lie outside the interval of periodicity for nearly circular Keplerian orbits. Let us demonstrate this by considering one example in more detail – namely, the 6-step implicit method SZ6i defined by (71) and (73). This is the most susceptible to resonant instabilities of the zero-growth methods we have examined, both because it has the largest interval of periodicity and because, as $u_1 \rightarrow -1$, two of the spurious roots coalesce as $u_1 \rightarrow -1$. We recall that there are five spurious roots on the unit circle, namely $\xi_2 = -1$, and the two complex-conjugate pairs $\xi_{3,4} = u_1 \pm iv_1$ and $\xi_{5,6} = u_2 \pm iv_2$, where $v_j = (1 - u_j^2)^{1/2}$. Using (71), the angular separations between the spurious roots on the unit circle can be readily computed as a function of u_1 . Figure 9 shows the locations of the potentially troublesome timesteps h , together with the maximum possible timestep (already presented in Figure 3). The resonant instabilities always occur at timesteps that are outside the interval of periodicity for Keplerian orbits. Similar results hold for the methods SZ5 and SZ6e.

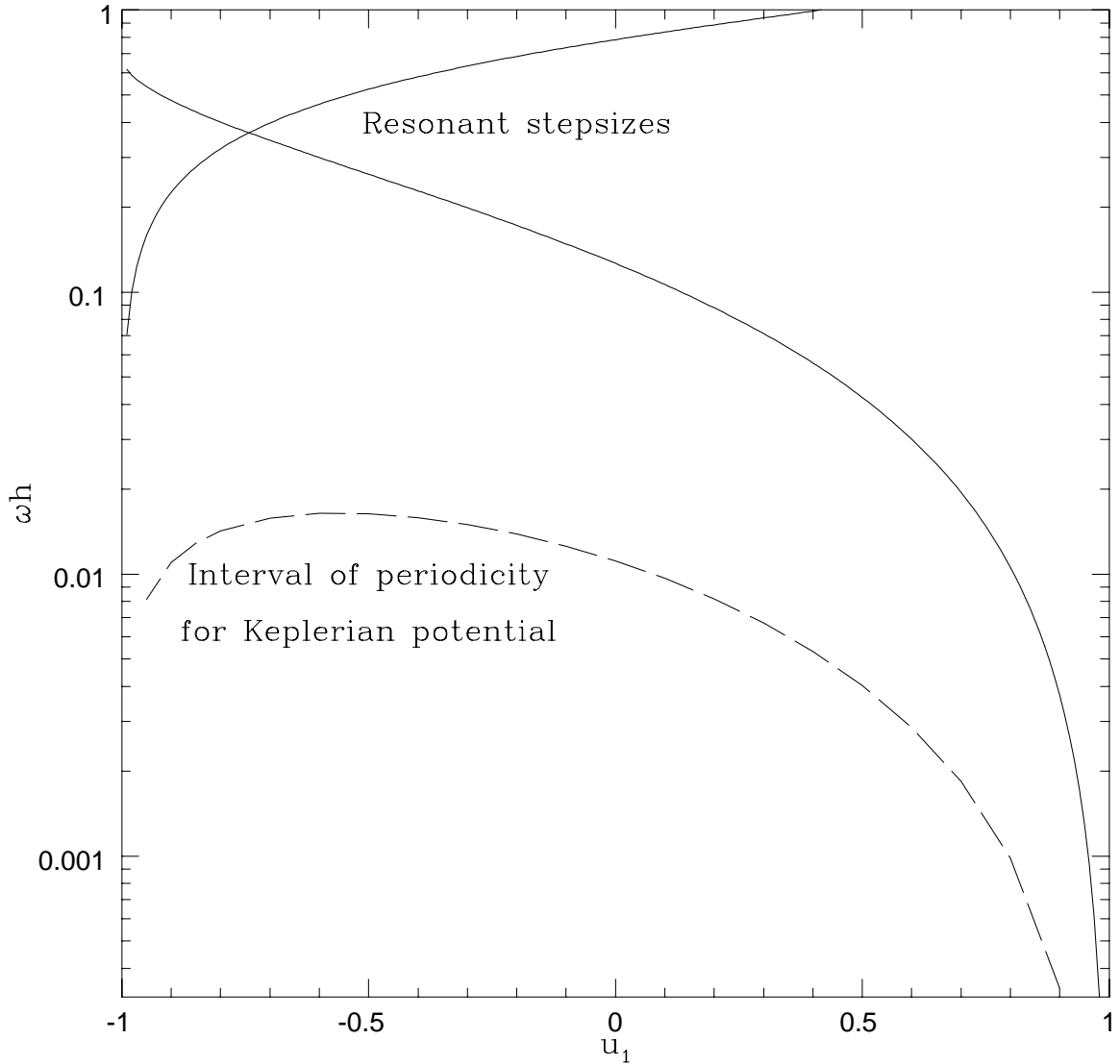


Fig. 9.— For the 6-step implicit method SZ6i, the resonant timesteps are shown in the full lines. The interval of periodicity for nearly circular Keplerian orbits is shown in a dashed line. The resonant timesteps are always larger than the maximum permitted timestep. Similar results hold true for SZ5 and SZ6e.

5. Conclusions

The generic instabilities of multistep RIAs for first-order differential equations identified by Cano & Sanz-Serna (1998) are a grave problem and render many of these methods unusable. The main contribution of this paper is the elaboration of a class of multistep RIAs – the zero-growth methods – that successfully evade the instabilities. This select group includes two familiar second-order multisteps, namely the trapezoidal method (54) and the explicit midpoint method (58), as well as entirely new multistep RIAs. In particular, we have identified three one-parameter families of zero-growth, fourth-order RIAs – namely, the five-step implicit method SZ5 defined by equations (68) and (69), the six-step implicit method SZ6i defined by (71) and (73), and the six-step explicit method SZ6e defined by (74) and (76). Of these, the explicit method SZ6e eliminates the need to iterate to convergence at each timestep without a major sacrifice in the interval of periodicity. The stability of the zero-growth methods has been understood at a theoretical level and confirmed at a practical level by integrations of circular and eccentric Keplerian orbits.

There are several advantages of multistep RIAs for first-order differential equations over the multistep RIAs for special second-order differential equations examined by Lambert & Watson (1976), Quinlan & Tremaine (1990), and Fukushima (1998, 1999). They permit the introduction of variable timesteps without spoiling reversibility or long-term energy conservation. They are also more general, since any ordinary differential equations can always be reduced to a system of first-order equations; thus, for example, the methods described here can be used to follow orbits in rotating frames of reference or the motions of rotating rigid bodies. A third advantage is that they are less susceptible to timestep resonances. The price paid for these attractive features is that (i) the interval of periodicity of the higher order methods such as SZ5, SZ6i and SZ6e is rather small, forcing the use of smaller timesteps than other methods; (ii) more steps are needed for a method of given order; there are no fourth-order methods with fewer than five steps and no fifth or sixth-order methods with 8 or fewer steps (the limit of our explorations). Nonetheless, the six-step explicit method (SZ6e) remains a competitive option for problems in which it is critical to have variable timesteps and to avoid irreversible numerical errors: examples include long-term integrations of asteroid or comet orbits, or orbits near the centers of galaxies.

There are several possible avenues for future exploration:

1. Are there zero-growth RIAs with more than $k = 6$ steps that have higher order or a larger interval of periodicity? We have explored all $k \leq 8$ but have found no RIAs of order greater than 4.
2. Gautschi (1961) developed a class of methods closely related to the linear multisteps.

Just as a linear multistep is defined by the requirement that the operator (23) annihilate all algebraic polynomials of order $\leq p$, so the Gautschi multisteps annihilate certain trigonometric polynomials up to a given degree. These methods are particularly appealing when the solution is known to be periodic and a reasonable estimate for the period of the orbit can be guessed in advance – requirements that are often satisfied in solar system integrations. Can we find reversible Gautschi multisteps?

3. Integration methods are generally designed to maximize the order p , defined so that the one-step error in following a system with characteristic frequency ω is proportional to $(h\omega)^{p+1}$. Perhaps it is more sensible to “economize” the error, by minimizing the maximum value of the error over a range of frequencies $0 < \omega \leq \omega_{\max}$. In this case the error would be nearly proportional to a Chebyshev polynomial $T_{p+1}(x)$ with argument $x = \omega/\omega_{\max}$ and degree $p + 1$, instead of x^{p+1} .

We are indebted to Gerry Quinlan for communicating his results on resonant instabilities in advance of publication. This research was supported in part by NASA grant NAG5-7310. NWE thanks both the Canadian Institute for Theoretical Astrophysics and the Department of Astrophysical Sciences, Princeton University for their hospitality during working visits. His research is supported by the Royal Society.

REFERENCES

Arnold, V.I. 1984, in Nonlinear and Turbulent Processes in Physics, 3, ed. R.Z. Sagdeev (Chur: Harwood), 1161

Calvo, M.P., López-Marcos, M.A., & Sanz-Serna, J.M. 1998, App. Num. Math. 28, 1

Cano, B. 1996, Ph. D. thesis, University of Valladolid

Cano, B., & Sanz-Serna, J.M. 1998, IMA Journal of Numerical Analysis 18, 57

Channell, P.J., & Scovel, J.C. 1990, Nonlinearity 3, 231

Davies, P.C.W. 1974, The Physics of Time Asymmetry (Berkeley: University of California Press)

Fukushima, T. 1998, in Proceedings of the 30th Symposium on Celestial Mechanics, eds T. Fukushima, T. Ito, T. Fyse & H. Umemura (Kanagawa, Japan), 229

Fukushima, T. 1999, in Proceedings of IAU Colloquium 173, in press

Gautschi, W., 1961, *Numer. Math.*, 3, 381

Gear, C.W. 1971, *Numerical Initial Value Problems in Ordinary Differential Equations* (Englewood Cliffs: Prentice-Hall)

Henrici, P. 1962, *Discrete Variable Methods in Ordinary Differential Equations* (New York: Wiley)

Hockney, R.W. & Eastwood J.W. 1981, *Computer Simulation Using Particles* (London: McGraw-Hill)

Huang, W., & Leimkuhler, B. 1997, *SIAM J. Sci. Comput.* 18, 239

Hut, P., Makino, J., & McMillan, S. 1995, *Astrophys. J.*, 443, L93

Hut, P., Funato, Y., Kokubo, E., Makino, J., & McMillan, S. 1997, in *Computational Astrophysics: 12th Kingston Meeting on Theoretical Astrophysics*, eds. D. A. Clarke & M. J. West (San Francisco: Astronomical Society of the Pacific), 26

Kang, F. 1986, *J. Comp. Math.* 4, 279

Lambert, J.D. 1973, *Computational Methods in Ordinary Differential Equations* (New York: Wiley)

Lambert, J.D., & Watson, I.A. 1976, *J. Inst. Maths Applics.* 18, 189

Marsden, J., Patrick, G., & Shadwick, W. F., eds. 1996, *Integration Algorithms for Classical Mechanics*, Fields Institute Communications, 10, 217

Mikkola, S. 1997, *Celest. Mech. Dyn. Astr.* 67, 145

Moser, J., 1973, *Stable and Random Motions in Dynamical Systems* (Princeton: Princeton University Press)

Quinlan, G.D. 1999, [astro-ph/9901136](http://arxiv.org/abs/astro-ph/9901136)

Quinlan, G.D., & Tremaine, S. 1990, *Astron. J.* 100, 1694

Quinn, T.R., Katz, N., Stadel J. & Lake G. 1997, [astro-ph/9710043](http://arxiv.org/abs/astro-ph/9710043), submitted to *Astrophys. J.*

Ralston A. & Rabinowitz P. 1978, *A First Course in Numerical Analysis* (London: McGraw-Hill)

Roberts, J.A.G., & Quispel, G.R.W. 1992, Physics Reports 216, 63

Sanz-Serna, J.M. & Calvo M.P. 1994, Numerical Hamiltonian Problems (London: Chapman and Hall).

Yoshida, H. 1993, Celest. Mech. Dyn. Astron. 56, 27